Materials Research Proceedings 54 (2025) 772-779 https://doi.org/10.21741/9781644903599-83

Comparison of different machine control modes during friction extrusion of AA2024

Harikrishna Rana[1,a *], Chang Chan[2,b], Uceu F.H. Suhuddin[2,c], Noomane Ben Khalifa[1,2,d], Benjamin Klusemann[1,2,e]

[1]Leuphana University of Lüneburg, Institute of Production Technology and System, Universitätsallee 1, 21335 Lüneburg, Germany

[2]Helmholtz-Zentrum Hereon, Institute of Material and Process Design, Solid State Materials Processing, Max-Planck-Str. 1, 21502 Geesthacht, Germany

[a]harikrishasinh.rana@leupahan.de, [b]chang.chan@hereon.de, [c]uceu.suhuddin@hereon.de, [d]noomane.ben_khalifa@leuphana.de, [e]benjamin.klusemann@leuphana.de

Keywords: Friction Extrusion, Aluminum, Displacement-Control, Force-Control

Abstract. The friction extrusion process has recently been explored for manufacturing extrudates with unique microstructures and improved material properties. The process can be classified as a severe plastic deformation (SPD) process in which the compressive shear strains and friction-induced heat play a key role in achieving an intensely refined microstructure. The microstructure can be orchestrated by distinctive heating and plastic deformation conditions from different process parameters, viz. extrusion force, extrusion speed, spindle rotation speed, etc. Notably, the process dynamics lead to different strains and temperatures across the traverse and longitudinal sections of the extrudates, eventually resulting in distinctive microstructures. The present work focuses on comparing the responses of two different machine control modes viz., force and displacement control. The extrudate produced using displacement-control mode exhibited superior process stability, whereas force-control mode resulted in a more unstable process characterized by fluctuating spindle torques, varying extrusion speeds, and elevated temperatures, ultimately leading to lower extrudate quality. These process variabilities were reflected in the microstructures of the extrudates, particularly in the grain structures and defect formations.

Introduction

Over the past two decades, numerous researchers have focused on SPD processes for their ability to enhance mechanical properties through significant grain refinement without changing the material's chemical composition. [1]. Among various methods, Friction Extrusion (FE) is being reported for producing exudates with highly refined microstructures irrespective of the precursor material forms, including ingots, metal powders, chips, flakes, etc. [2–4]. The FE process is carried out by plunging a non-consumable die into a rotating container comprising billet material. As the container walls confine the billet material, its relative motion with the die generates frictional heat and compressive shear strains, resulting in the backward extrusion of wires with a highly refined microstructure.

Al-Cu-Mg alloys, recognized for their applications in aerospace and structural industries due to their precipitation-hardening properties, pose significant challenges during the extrusion process. Notably, the high copper content in these alloys decreases hot workability and increases the risk of hot cracking [5]. Hence, it is imperative to optimize temperature and strain rates during extrusion to control the thermal stresses and material flow. Additionally, the combination of high yield strength and low ductility makes it challenging to extrude this alloy at low extrusion forces or high extrusion rates. To address this, higher preheating temperatures are typically recommended during conventional extrusion lowering the material flow stresses [6]. However, excessive

preheating increases the susceptibility of the material to hot cracking. Since these alloys are challenging for conventional extrusion, FE could be an effective technique as demonstrated by Whalen et al. [7] for AA 7075 alloy tube extrudates. Further, Baffari et al. [8] successfully extruded AA 2050 alloy using FE, irrespective of the initial temper conditions reporting highly refined and equiaxed microstructure across the extrudate. Tang and Reynolds [9] reported the successful FE of AA 2050 and AA 2195 alloys, noting that the process window was constrained by extrusion temperatures, which increased the risk of cold tearing or hot cracks. Further, considerably more dynamic nature of the FE process compared to conventional extrusion, compelled by the high in-process variability of friction conditions and torque, adds to its complexity. In a nutshell, the FE of high-strength aluminum alloys requires a comprehensive understanding of process characteristics, leading to the capability to control the process behavior.

The present study describes the process characteristics, extrudate quality and microstructures resulting from two different machine control modes viz., force and displacement-control. Such knowledge can be an important feed for the scientific community for exploring the FE in high-strength aluminium alloys.

Materials & Methodology

Experiments were conducted on a special-purpose friction extrusion machine FE 100 (Bond Technologies Inc., USA). AA2024 - T351 solid circular billets of 50 mm diameter were extruded to 10 mm diameter wires using a scroll die with a constant extrusion ratio of 25. The experimental campaign was divided into two machine control modes, namely force-control mode and displacement-control mode, to study the influence of each one on the extrudate quality. The process evaluations were carried out in terms of control parameters and response variables. For instance, the first experiment was carried out with extrusion force and spindle rotation as control parameters while die advance velocity, temperature, and spindle torque represent the machine responses. Whereas the second one was executed with die advance velocity and spindle rotation as control parameters, and extrusion force, temperature, and spindle torque as machine responses. The employed process parameters are listed in Table 1. The temperatures during each process were recorded using a K-type thermocouple mounted 1 mm beneath the die face at a radius of 16.5 mm. The process cutoff was set at 525 °C, based on prior experiments showing that the extrudate started cracking above this temperature. Further, transverse and longitudinal sections were sliced, ground, and polished in colloidal silica for metallographic analysis. The prepared specimens were electrically etched with Barker's solution and analyzed using a Keyence VHX-600 digital microscope and a Leica DMi8 optical microscope (OM) under polarized light to infer the grain sizes in different regions as per ASTM E112-3. The non-extruded residual feedstocks left in the container after FE were also sectioned and analyzed with OM to infer the transition zones.

Table 1 – Summary of process parameters used for the experimental campaign

Experiment ID	Spindle rotation speed (RPM)	Machine Control Mode	Extrusion Force (kN)	Die Advance Velocity (mm/min)
A	90	Force	200	-
B		Displacement	-	9

Results & Discussions

Process Behavior. Fig. 1 exhibits the comparison between force-control mode and displacement-control mode experiments through various control parameters and response variables during the extrusion phase of FE.

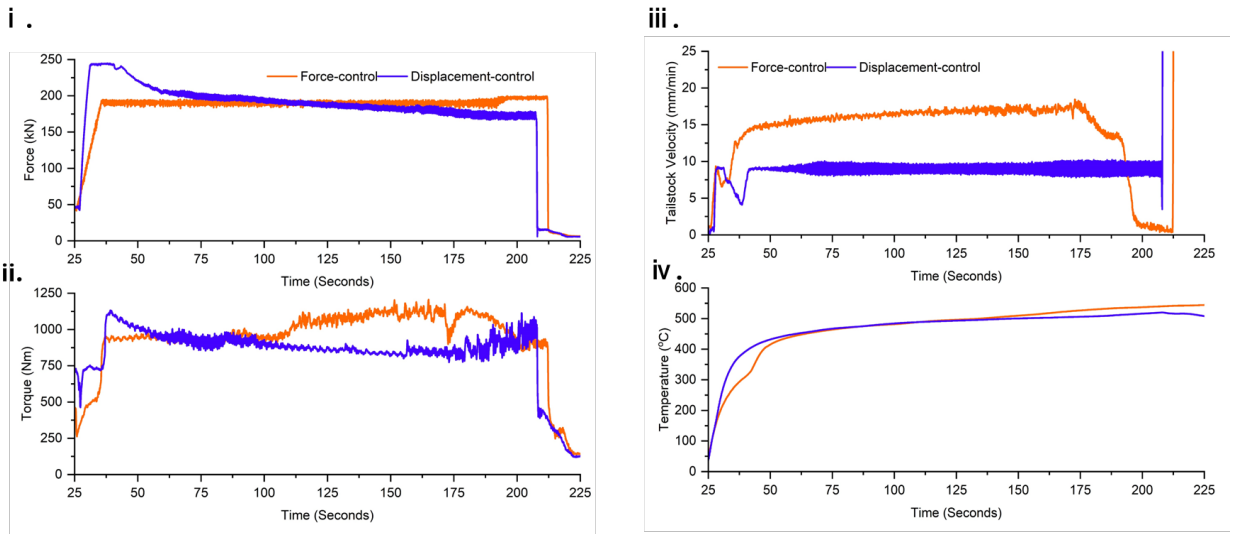

Figure 1 – Process plots showing the comparison between force-control mode and displacement-control mode during the extrusion phase through (i.) Extrusion Force (ii.) Torque (iii.) Tailstock Velocity (iv.) Temperature

FE process comprises four steps: *a.* Preheating *b.* Ramping *c.* Extrusion *d.* Retraction. Once the die contacts the solid billet in a rotating container, the preheating is carried out at low force (~ 50 kN) to ensure uniform heating of the billet. Further, based on the selected machine control mode, the target spindle rotation and extrusion force in force-control mode, or the spindle rotation and die advance velocities in displacement-control mode, are approached gradually in the ramping phase to prevent abrupt changes in the parameters. During the extrusion phase, in force-control mode, the controller adjusts the die advance velocity to maintain the desired extrusion force, whereas in displacement-control mode, it adjusts the extrusion force to sustain the target die advance velocity. It is observed that as the temperature increases during the extrusion phase, the die advance velocity gradually rises over time in force-control mode, while in displacement-control mode, the extrusion force decreases over time due to material softening. The extrusion force was limited by 250 kN, explaining the initial drop in terms of die velocity until sufficient heat is created and the force decays to a value around 200 kN during the extrusion phase, which allows for a fair comparison between both processes of the different control mode (see, Fig. 1 (i)).

The prime factors affecting the quality of the output product in SPD processes are temperature and strain rates, which complement each other. Likewise, during the extrusion phase of FE, the uniformity of properties along the extrusion length can be achieved by uniform torque, temperature stability, and smaller gradients to have consistent extrudate quality. Nevertheless, the dynamic nature of torque, friction conditions, temperature, etc. makes FE a quite complex process as compared to the conventional extrusion process. The spindle torque, temperature, and extrusion force or die advance velocity are of particular interest while evaluating the process performance. To evaluate further, Table 2 summarizes the response variables for both process conditions, which will be elaborated in the following sections.

Spindle Torque and Extrusion Force. Unlike conventional extrusion, the energy input for the FE process is induced mechanically through spindle rotation and hydraulic drive responsible for the extrusion force [10,11]. The spindle torque increases with the resistance to spindle rotation caused by the feedstock during the process, as well as by the spindle's rotation (which was maintained constant in all experiments in this study). The experiment performed in force-control mode shows a significantly higher average die advance velocity compared to the experiment in displacement-control mode, wherein it was fixed.

Moreover, the experiment in displacement-control mode exhibits fewer fluctuations in the spindle torque values compared to the force-control mode, indicating more stable friction and shearing conditions. During force control mode a gradual rise in die advance velocity can be noticed which can be attributed to the softening induced by corresponding temperature rise over time. As the controller maintains a constant extrusion force, any mismatch between the rate of rise in die advancement velocity and temperature translates into variations in torque values. When the temperature rise is inadequate, the colder feedstock material possessing higher flow stresses, offers higher resistance to plastic deformation and the spindle rotation, causing torque spikes. Conversely, when the rate of temperature rise surpasses that of die advance velocity, relatively hotter material provides less resistance, resulting in lower torque values. Given the importance of temperature evolution in process dynamics, a detailed analysis of temperature trends is presented in the following section.

Table 2 – Summary of response variables resulting from different process parameters

Exper-iment ID	Peak Torque (Nm)	Peak Force (kN)	Die Advance Velocity[#] (mm/min)	Extrudate Length (cm)	Temperature T_0 (°C)	Temperature Difference ($T_0 - T_{71}$) [##] (°C)	Extrusion time for EL_{71} [###] (Second)	Temperature rise /cm-second (°C/cm-S)
A	1,205	200	~16	111	308	220	104	0.029
B	1,066	240	9	71	305	197	176	0.019

[#]Symbol "~" signifies the average value during the extrusion phase, [##]$T_{0:}$ Temperature at the start of extrusion phase; T_{71} :Temperature after 71 cm of extrudate length; [###]EL_{71}.: Extrudate Length of 71 *cm.*

Temperature. Fig. 2 compares the temperature variations over time and space during the extrusion phase for both FE experiments using force and displacement control modes. Notably, the temperature maps vary differently in the two domains. In the time domain, the force-control experiment exhibits a steeper slope after 100 seconds, while in the space domain, the displacement-control experiment shows consistently higher temperatures up to an extrusion length of 71 cm. Therefore, it can be presumed that an accurate assessment of the temperature behaviour during FE can only be done by considering the combined results from both, time and space domains. The temperature differences from the start of the extrusion phase (T_0) to an extrudate length of 71 cm (T_{71}), along with the time spent, are listed for clarity in Table 2. The force-control experiment data revealed that the temperature increase per unit of time and length is comparatively higher than that observed in the displacement-control experiment. The higher temperature values may indicate greater energy input during the process, as the force-control experiment has demonstrated consistently higher torque values. Ultimately, such varying energy inputs along with the resulting temperature and strain rates, have a profound impact on the macrostructural and microstructural characteristics.

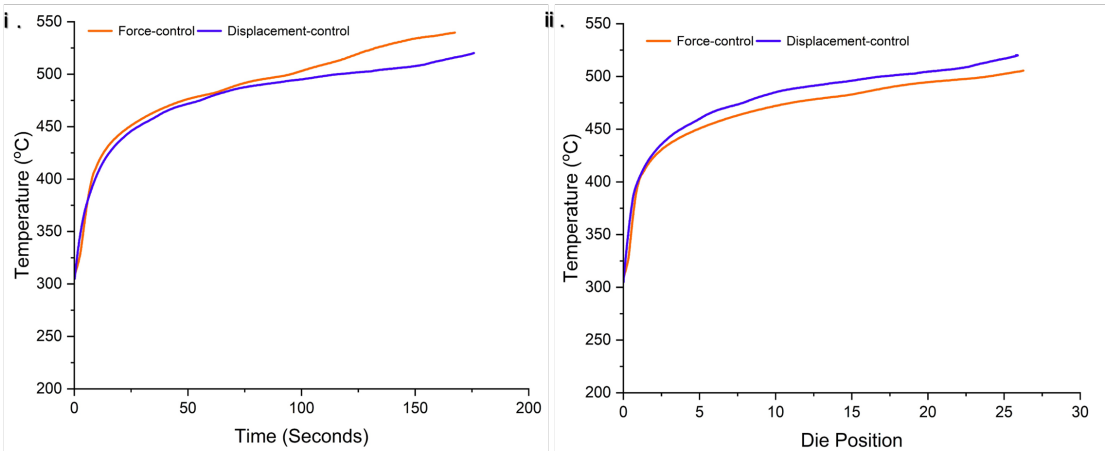

Figure 2 – Temperature maps, exhibiting a comparison between force and displacement-control mode during the extrusion phase over the (i)Time and (ii)Space.

Microstructural Characteristics. Fig. 3 displays the optical micrographs of extrudate B, demonstrating material flow patterns, and grain structures in different zones namely i. Base material (BM) ii. Thermo-mechanically affected zone 1 (TMAZ 1) iii. TMAZ 2 iv. Extrudate. The BM region was characterized by typically elongated grains whereas TMAZ 1 which is next to the BM region, was characterized by a deformed grain structure. Further upward in the direction of extrudate, TMAZ 2 and extrudate regions comprised of intensively refined grain structure. The present grain characteristics were consistent with past studies conducted by the authors [2]. Nevertheless, the central regions of the extrudate are characterized by a narrow column (≈700 – 1100 µm) of elongated grains enveloped by intensely refined grains (≈ 4 - 6 µm) towards the periphery.

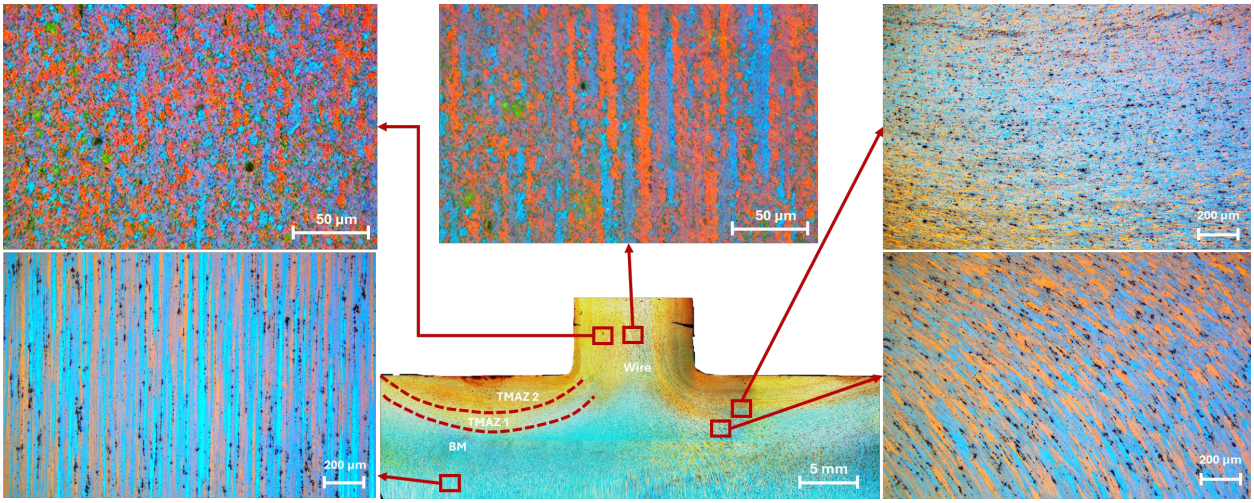

Figure 3 – Optical micrographs of extrudate B (displacement-control mode) with billet exhibiting grain structures in different zones

The macro and micrographs of both extrudates are displayed in Fig. 4. The force-control extrudate was characterized by annular cracks on its outer surface after 160 cm as shown in Fig. 4 (i). A similar cracking was reported while FE of Al–Cu–Li–Mg–Ag alloys from chips [9]. Although the displacement-controlled extrudate displayed an almost flawless macrostructure and microstructure resulting from stable process behaviour, the final ~ 5 cm showed a few annular cracks due to the extremely high temperatures at the end. Furthermore, abnormal grain growth is visible near the cracks in the force-control extrudate, indicating the adiabatic deformation phenomenon reported by Bhaduri et al. [12] in the course of conventional extrusion.

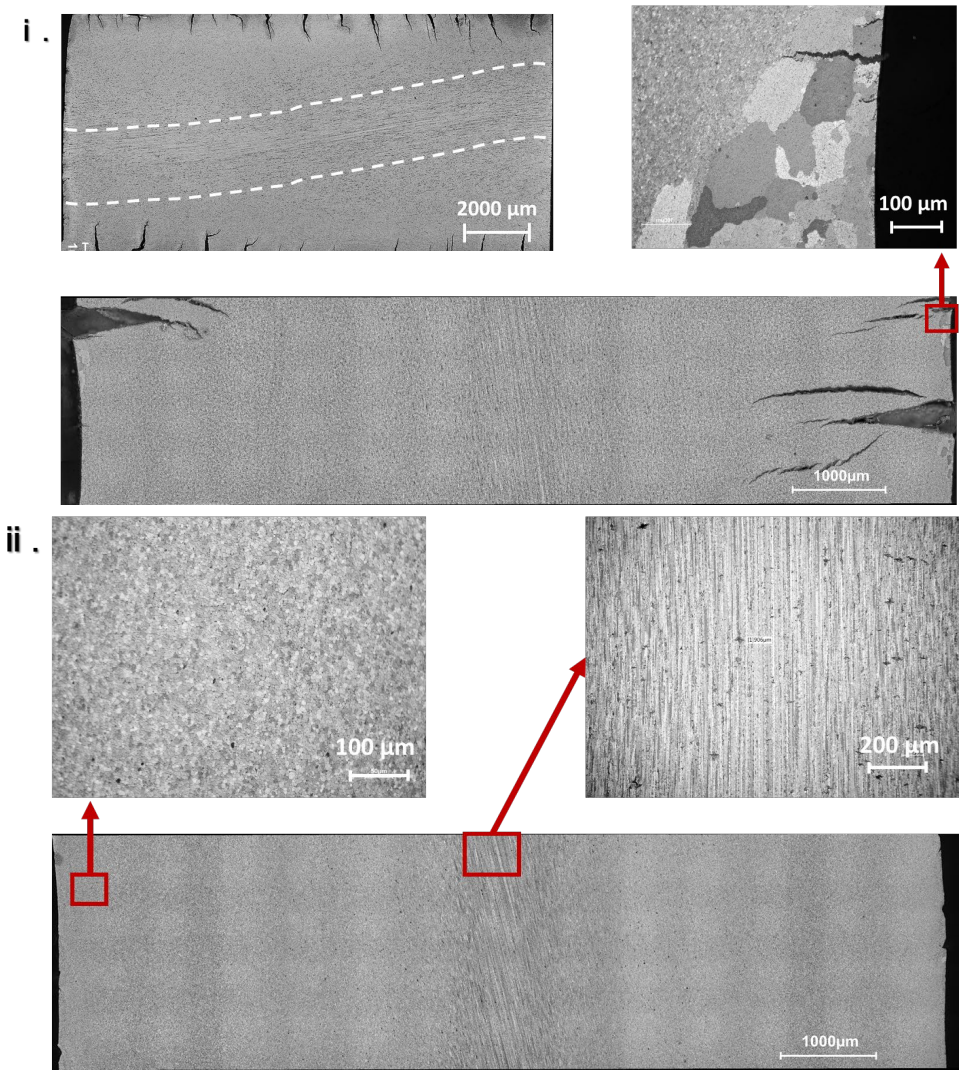

Figure 4 – Optical micrographs displaying grain structures in different regions of extrudate produced with i. Force-control mode ii. Displacement-control mode.

Apart, elongated grains are visible in the central region of both extrudates, demonstrating the lack of adequate recrystallisation and can be attributed to the lower plastic strain values as compared to the progressive position towards the periphery [13]. The displacement control extrudate displayed a slightly narrow region of elongated grains, see Fig. 5. Notably, force-control extrudate exhibited the elongated grains, slightly deflected from the center, see Fig. 4 (i). Since crack formation during extrusion alters the stress distribution across the extrudates, thereby shifting the strain fields, leading to the deflection of elongated grains, which corresponds to the patterns of the hot cracks. However, the displacement-control extrudate exhibited elongated grains nearly parallel to the extrusion direction, see Fig. 4 (ii).

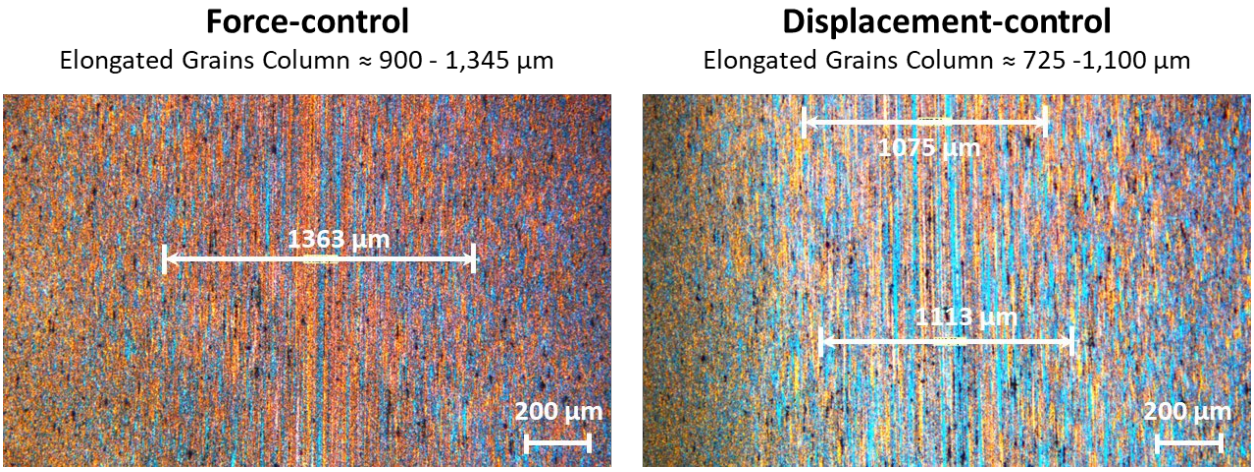

Figure 5 – Optical micrographs comparing dimensions of elongated grain column in the central region of force-control and displacement-control extrudates

Conclusions and Summary

From the current set of experiments, better process characteristics were observed in the displacement-control mode owing to stable process and response variables. Force-control mode resulted in higher average die advance velocities and a greater temperature rise per unit time and space, causing instability during the process from mid-way to the end. Sudden toque bumps recorded with force-control mode resulted mostly in surface defects and lower extrudate quality. The intermittent spindle torque spikes were greatly avoided during displacement-control mode owing to stable temperature characteristics. All the extrudates were characterized by intensely refined microstructure but a narrow central region (~7-12% of total diameter) of elongated grains, resulting from the lower plastic strain values in the center as compared to the periphery. Comparatively wider regions were visible for the extrudates prepared in force-control mode.

Funding

This project has received funding from the European Research Council (ERC) under the European. Union's Horizon 2020 research and innovation program (grant agreement No 101001567).

References

[1] R.Z. Valiev, N.A. Krasilnikov, N.K. Tsenev, T.G. Langdon, Plastic deformation of alloys with submicron-grained structure, Prog Mater Sci 137 (2006) 881–981. https://doi.org/10.1016/0921-5093(91)90316-F

[2] U.F.H. Suhuddin, L. Rath, R.M. Halak, B. Klusemann, Microstructure evolution and texture development during production of homogeneous fine-grained aluminum wire by friction extrusion, Mater Charact 205 (2023) 1-13. https://doi.org/10.1016/j.matchar.2023.113252

[3] L. Rath, U.F.H. Suhuddin, B. Klusemann, Comparison of Friction Extrusion Processing from Bulk and Chips of Aluminum-Copper Alloys, 926 (2022) 471–480.

[4] X. Li, C. Zhou, N. Overman, X. Ma, N. Canfield, K. Kappagantula, J. Schroth, G. Grant, Copper carbon composite wire with a uniform carbon dispersion made by friction extrusion, J Manuf Process 65 (2021) 397–406.

[5] S.A. Whalen, K.S. Kappagantula, X. Li, N.R. Overman, M.J. Olszta, T. Wang, D.R. Herling, S.R. Suffield, T.J. Roosendaal, B.S. Taysom, Shear assisted processing and extrusion (shape) of aluminum alloy 7075, 2024, and al-12.4 tm, Pacific Northwest National Lab.(PNNL), Richland, WA (United States) (2021).

[6] V.N.S.U. Viswanath Ammu, I. Raju, R.N. Chouhan, A. Agnihotri, Effect of ram speed on surface quality and mechanical properties during extrusion of AA2024 alloy, Mater Today Proc 113 (2024) 258–263. https://doi.org/https://doi.org/10.1016/j.matpr.2023.09.146

[7] S. Whalen, M. Olszta, M. Reza-E-Rabby, T. Roosendaal, T. Wang, D. Herling, B.S. Taysom, S. Suffield, N. Overman, High speed manufacturing of aluminum alloy 7075 tubing by Shear Assisted Processing and Extrusion (ShAPE), J Manuf Process 71 (2021) 699–710.

[8] D. Baffari, A.P. Reynolds, X. Li, L. Fratini, Influence of processing parameters and initial temper on Friction Stir Extrusion of 2050 aluminum alloy, J Manuf Process 28 (2017) 319–325.

[9] W. Tang, A.P. Reynolds, Production of wire via friction extrusion of aluminum alloy machining chips, J Mater Process Technol 210 (2010) 2231–2237.

[10] M. Reza-E-Rabby, X. Li, G. Grant, S. Mathaudhu, A. Reynolds, Process parameters and system responses in friction extrusion, J Manuf Process 85 (2023) 21–30. https://doi.org/10.1016/j.jmapro.2022.11.027

[11] K.N. Salloomi, L.A. Sabri, Y.M. Hamad, S.N. Mohammed, 3-Dimensional nonlinear finite element analysis of both thermal and mechanical response of friction stir welded 2024-T3 aluminium plates, Journal of Information Engineering and Applications 3(9) (2013) 6–15.

[12] A. Bhaduri, Mechanical properties and working of metals and alloys, Springer, 264 (2018) 599-646, https://doi.org/10.1007/9

[13] G. Diyoke, L. Rath, R. Chafle, N. Ben Khalifa, B. Klusemann, Process simulation of friction extrusion of aluminum alloys, in: Materials Research Proceedings, Association of American Publishers, 28 (2023) 487–494. https://doi.org/10.21741/9781644902479-53